Biochemical and Biophysical Research Communications 434 (2013) 217–222

Contents lists available at SciVerse ScienceDirect

Biochemical and Biophysical Research Communications

journal homepage: www.elsevier.com/locate/ybbrc

Oxidized silicon nanoparticles for radiosensitization of cancer and tissue cells

Stefanie Klein [a], Maria L. Dell'Arciprete [b], Marc Wegmann [a], Luitpold V.R. Distel [c], Winfried Neuhuber [d], Mónica C. Gonzalez [b], Carola Kryschi [a,*]

[a] Department Chemistry and Pharmacy, Physical Chemistry I and ICMM, Friedrich-Alexander University of Erlangen-Nuremberg, Egerlandstr. 3, D-91058 Erlangen, Germany
[b] Instituto de Investigaciones Fisicoquímicas Teóricas y Aplicadas (INIFTA), Facultad de Ciencias Exactas, Universidad Nacional de La Plata, Casilla de Correo 16, Sucursal 4, 1900 La Plata, Argentina
[c] Department of Radiation Oncology, Friedrich-Alexander University of Erlangen-Nuremberg, Universitätsstr. 27, D-91054 Erlangen, Germany
[d] Department of Anatomy, Chair of Anatomy I, Friedrich-Alexander University of Erlangen-Nuremberg, Krankenhausstr. 9, D-91054 Erlangen, Germany

ARTICLE INFO

Article history:
Received 10 March 2013
Available online 25 March 2013

Keywords:
Silicon nanoparticles
Radiosensitizer
Oxidative stress
Reactive oxygen species

ABSTRACT

The applicability of ultrasmall uncapped and aminosilanized oxidized silicon nanoparticles (SiNPs and NH_2-SiNPs) as radiosensitizer was studied by internalizing these nanoparticles into human breast cancer (MCF-7) and mouse fibroblast cells (3T3) that were exposed to X-rays at a single dose of 3 Gy. While SiNPs did not increase the production of reactive oxygen species (ROS) in X-ray treated cells, the NH_2-SiNPs significantly enhanced the ROS formation. This is due to the amino functionality as providing positive surface charges in aqueous environment. The NH_2-SiNPs were observed to penetrate into the mitochondrial membrane, wherein these nanoparticles provoked oxidative stress. The NH_2-SiNPs induced mitochondrial ROS production was confirmed by the determination of an increased malondialdehyde level as representing a gauge for the extent of membrane lipid peroxidation. X-ray exposure of NH_2-SiNPs incubated MCF-7 and 3T3 cells increased the ROS concentration for 180%, and 120%, respectively. Complementary cytotoxicity studies demonstrate that these silicon nanoparticles are more cytotoxic for MCF-7 than for 3T3 cells.

1. Introduction

In the recent past intense research activities were focused onto the development of silicon nanoparticles as photosensitizer of singlet oxygen generation for photodynamic therapy [1,2]. The applicability of the photodynamic therapy is limited to the treatment of superficial tumors due to the small penetration depth of visible light as well as the short diffusion path and short lifetime of singlet oxygen [3].

In case of ionizing radiation, such as X-rays or gamma rays, the penetration depth can be easily optimized to the range of 8–14 cm. Therefore, approximately half of the patients, who develop cancer, receive radiotherapy as a main component of their treatment. Radiotherapy uses X-rays for targeted destruction of malignant cells. X-rays may act directly on cellular material through either ionizing or exciting or indirectly, via interactions with molecules by generating free radicals that in turn can damage DNA or cellular organelles. However, there are various tumors that are hardly responsive or even resistant to radiotherapy. One goal of radiotherapy is to enhance the radiotherapeutic efficacy for cancer to minimize its harmful effects on normal tissues. Therefore radiosensitizers have been developed which increase the sensitivity of tumor cells to X-ray radiation [3]. A recent *in vitro* study revealed that surface-oxidized silicon nanoparticles may increase the impact of X-radiation on the formation of reactive oxygen species (ROS) for clinically relevant doses [4]. Under ambient conditions silicon nanoparticles form an amorphous SiO_x shell (with $x < 2$). The SiO_x shell is considered to enhance X-ray induced generation of oxygen radicals ($OH^{\cdot}$, $HO_2^{\cdot}$, O_2^{-}) in aqueous solutions. Moreover, singlet oxygen is generated in X-ray treated solutions containing surface-stabilized, oxidized silicon nanoparticles [5].

Silica nanoparticles (SiO_2NPs) were reported to induce oxidative stress in a dose-dependent manner which was proven by the formation of ROS, lipid peroxidation (LPO) and depletion of glutathione (GSH) [5,6]. Molecular oxygen was observed to react with the fractured silica surface, where both, homolytic ($Si^{\cdot}$, $SiO^{\cdot}$) and heterolytic (Si^{+}, SiO^{-}) cleavage of the silicon–oxygen bond may take place [7]. The mechanism of intracellular ROS generation in the presence of SiO_2NPs presumably involves both, the mitochondrial respiration and the NAD(P)H oxidase system [8].

Coating of SiO_2NPs surfaces or those of oxidized silicon nanoparticles with suited organic groups was observed to suppress the SiO_2 or SiO_x induced ROS generation and is hence required for the development of biocompatible and biodegradable silicon nanoparticles for medical application [6]. Therefore they may be

* Corresponding author. Fax: +49 91318528967.
E-mail address: carola.kryschi@fau.de (C. Kryschi).

0006-291X/$ - see front matter © 2013 Elsevier Inc. All rights reserved.
http://dx.doi.org/10.1016/j.bbrc.2013.03.042

covered with detergents [9] or phospholipid micelles [10]. Otherwise, silicon nanoparticles can be functionalized with ethenyl derivatives that provide surface charges in aqueous environment due to their terminal amino (NH_2), azide (N_3) and carboxylic acid (COOH) groups [11]. The influence of surface charges on the cytotoxicity of such functionalized silicon nanoparticles was examined by Bhattacharjee et al. [12]. Positively charged silicon nanoparticles were observed to exhibit the highest cytotoxicity, since they significantly increase the intracellular ROS production.

In this contribution, the cellular uptake and influence of ultrasmall amino-silanized oxidized silicon nanoparticles (NH_2-SiNPs) and uncoated oxidized silicon nanoparticles (SiNPs) on the cell viability and oxidative stress were studied. The applicability of NH_2-SiNPs and SiNPs as radiosensitizer for X-rays in tumor cells was examined. Therefore these nanoparticles were internalized in human breast cancer (MCF-7) and mouse fibroblast (3T3) cells, which were exposed to X-radiation at a single dose of 3 Gy. The radioenhancement effect was assessed by measuring the intracellular ROS concentrations.

2. Materials and methods

2.1. Chemicals and instruments

Silicon tetrachloride (Aldrich, 99%), tetraoctylammonium bromide (TOAB, Aldrich, 98%) Aminopropyltriethoxysilane (APTES, Aldrich, ⩾98%,), $LiAlH_4$ (Fluka, >97%), toluene (VWR, 99.5%), cyclohexane (VWR, 100%) and methanol (VWR, p. a.) were used as received. KH_2PO_4 (p. a.) and K_2HPO_4 (99%) were purchased from Merck, NaCl (99.5%) from Fluka and Triton X-100 from Riedel-de Haën. DMEM, L-glutamine, FCS, penicillin–streptomycin-solution, sodium pyruvate, PBS, MEM, trypsin/EDTA, MTT (98%), trypanblue-solution (0.4%), sodium dodecylsulfate (SDS) (90%), Tris–HCl (99%), disodium EDTA (99%), trichloroacetic acid (TCA) (99%), 2-thiobarbituric acid (TBA) (98%), 5,5′-dithiobis(2-nitrobenzoic acid) (DTNB) (98%), 2′,7′-dichlorofluorescein diacetate (DCFH-DA) (95%) were purchased from Sigma–Aldrich and glutaraldehyde (25%) and potassium pyrophosphate from Roth. DCFH-DA was dissolved in dimethyl sulfoxide (DMSO) (99.7%, Baker) to obtain a stock solution (0.01 M) and was kept frozen at −20 °C. For loading the cells with DCFH-DA the stock solution was mixed with DMEM at a concentration of 100 μM.

The photoluminescence spectra of the NH_2-SiNP and SiNP colloids and DCF assay were recorded on a Horiba Jobin-Yvon FluoroMax-3 spectrofluorometer. Transmission electron microscopy (TEM) images of SiNPs were taking using a Zeiss EM 900 instrument that was operated at 80 kV accelerating voltage, and the cells were imaged using a Zeiss 906 transmission electron microscope (LEO, Oberkochen, Germany). The concentrations of the NH_2-SiNP and SiNP sample solutions were determined using ICP-AES, in order to prepare a cell culture medium that contains silicon at the concentration of 0.1 mg/ml. The MTT assay was measured at 590 nm using an Elisa microplate reader (Dynatech Laboratories, Inc.). The different cells experiments were irradiated using a 120 kV X-ray tube (Isovolt, Seifert, Ahrensberg, Germany). UV–Vis measurements were carried out using a Perkin Elmer Lambda 2 in the range of 300–700 nm.

2.2. Syntheses of SiNPs and NH_2-SiNPs

Silicon nanoparticles were synthesized using a reverse-micelle wet-chemistry procedure [13]. 0.63 g of TOAB was dispersed for 20 min in toluene using an ultrasonication bath. 0.63 mL of $SiCl_4$ was added to the solution and the sonication was maintained for another 20 min. Then 0.76 g of $LiAlH_4$ was added to the solution. After 30 min sonication, 30 mL of MeOH was slowly incorporated to the suspension to eliminate the excess of the reductant. In order to break the micelles, the mixture of solvents was evaporated, and the particles were dispersed in 30 mL of cyclohexane. Three liquid–liquid extractions were performed with 30 mL of water. Finally, the organic phase was evaporated and the particles were dispersed in 20 mL of toluene or water for the cell experiments.

The SiNPs were functionalized via silanization. The toluene suspension of the SiNPs was stirred for 24 h at reflux with 1.5 mL of APTES. Afterwards the suspension was evaporated, and 20 mL of water was added. The purification of the functionalized SiNPs was performed via dialysis. The aqueous suspension was put into a Serva Membra-Cell MWCO 7000 membrane, and the dialysis tubing was submerged in distilled water. After 4 h, the water was changed twice and the suspension was left overnight. Finally, the suspension was evaporated and the aminosilanized SiNPs (NH_2-SiNPs) were dispersed in toluene or water.

2.3. Cell culture

The MCF-7 and 3T3 cells were cultured in DMEM containing 4500 mg glucose/L, which was enriched with 10% fetal calf serum (FCS), 1 mM sodium pyruvate, 100 U/mL penicillin, 100 μg/mL streptomycin, 2 mM L-glutamine and 1% MEM nonessential amino acids. In a humidified environment of 5% CO_2 at 37 °C the cells were incubated and subcultivated twice a week.

2.4. Transmission electron microscopy (TEM)

MCF-7 and 3T3 cells were incubated with cell culture medium containing SiNPs or NH_2-SiNPs at a concentration of 0.1 mg Si/mL. Cells were washed with PBS and fixed with 2.5% glutaraldehyde overnight at 4 °C and then postfixed in 1% osmium tetroxide and 3% potassium ferricyanide at room temperature. Through-graded alcohols cells were dehydrated, embedded in Epon and mounted on Epon blocks. Uncontrasted silver-grey ultrathin sections were imaged.

2.5. Cell viability assay

The mitochondrial function and cell viability of the NH_2-SiNPs and SiNPs, TOAB and APTES were evaluated using the 3-(4,5-dimethylthiazol)-2-diphenyltetrazolium bromide (MTT) assay. The two different cell lines were seeded in a 96 well-plate at a density of 10^3 cells per well. After 3 days the cell culture medium was replaced with one containing TOAB (0.1 mg/mL), APTES (0.1 mg/mL), SiNPs or NH_2-SiNPs both at a concentration of 0.1 mg Si/mL. After 24, 48 and 72 h incubation 50 μL of MTT solution (0.5 mg/mL in PBS) was added. The solution was carefully removed after 1 h, and the formazan crystals were solubilized with 100 μL SDS (0.2 mg/mL)-HCl (0.02 M)-solution. The metabolic activity was determined by measuring the absorbance of the formazan solution at 550 nm.

2.6. Intracellular ROS measurement

MCF-7 or 3T3 cells were cultivated in 96 well-plates at a density of 10^3 cells per well and were allowed to grow over 3 days. After removing the medium, the cells were incubated for 24 h with cell culture media that contains SiNPs or NH_2-SiNPs (0.1 mg Si/mL). Afterwards the cells were washed with PBS and loaded with 100 μM DCFH-DA in DMEM for 30 min. Each well was loaded with PBS. One half of the plate was irradiated at a single dose of 3 Gy. Since the ROS oxidize intracellular DCFH to the fluorescent DCF dye, the DCF fluorescence intensity is taken as being directly proportional to the ROS concentration. The fluorescence emission

was excited at 480 nm, and its spectrum was recorded in the range of 500–700 nm. The relative fluorescence intensity was determined by integrating the spectra. The fluorescence intensity values were related to those obtained from fluorescence measurements of cells in culture medium.

2.7. Preparation of the cell extract

Both cell lines were cultured in 25 cm^2 flasks, exposed to SiNPs or NH_2-SiNPs (0.1 mg Si/mL) for 24 h. One half of the cell culture flasks were irradiated at a single dose of 3 Gy. The cells were harvested by treating with trypsin–EDTA at room temperature. The cell pellets were then lysed in cell lysis buffer (20 mM Tris–HCl (pH 7.5), 150 mM NaCl, 1 mM Na_2EDTA, 1% Triton, 2.5 mM potassium pyrophosphate). After centrifugation (15,000*g*, 10 min, 4 °C) the cell extract (supernatant) was maintained on ice.

2.8. Membrane lipid peroxidation

The level of membrane lipid peroxidation (LPO) was determined by measuring the formation of malondialdehyde (MDA) as a product of membrane LPO [14]. A mixture of 0.1 ml cell extract, 0.4 ml 0.1 M potassium phosphate buffer (pH 7.4), 0.75 ml 5% TCA and 0.75 ml 1% TBA was heated at 65 °C for 30 min. After cooling to room temperature the mixture was centrifuged (2300*g*, 15 min) to collect supernatant. The absorbance of the supernatant was measured at 532 nm and the concentration of MDA in nmole/mg protein was determined using the molar extinction coefficient of $1.56 \times 10^5\ M^{-1}\ cm^{-1}$.

2.9. Intracellular glutathione level

The gluthatione (GSH) concentration was determined using Ellman's method [15]. 0.1 mL cell extract was mixed with 0.9 mL 5% TCA and subsequently centrifuged (2300*g*, 15 min, 4 °C). 0.5 mL of the supernatant was added into 1.5 mL 0.01% DTNB solution. The absorption was measured at 412 nm and the amount of GSH was calculated in terms of nmole/mg protein.

2.10. Statistical analysis

Data are presented as arithmetic mean values ± standard error (SE). Statistical analysis was performed using the analysis of variance (ANOVA) with *post hoc* Bonferroni correction for multiple comparisons. A value of $p < 0.05$ was considered to be statistically significant.

3. Results

Fig. 1 shows the photoluminescence emission (PL) and excitation (PLE) spectra of toluene colloids of SiNPs (left) and NH_2-SiNPs (right). The PL spectrum of the SiNPs excited at 300 nm exhibits a broad band at 370 nm with a full width at half maximum of about 1 eV. The structural features of the PL and PLE spectra as well as the small PL quantum yields (<10%) of the SiNPs indicate both, a broad size distribution centered around 1 nm and sparsely oxidized surfaces that are presumably composed of Si–H, Si–OH, unsaturated Si atoms and SiO_x layer fragments [13,16]. In contrast, the PL spectrum of the NH_2-SiNPs has a multi-peak structure beginning at 405 nm with a mean peak separation of 1380 cm^{-1} (Fig. 1, right). This multi-peak structure appears independently of the excitation wavelength and is thus attributed to a vibronic structure due to a mixture of LO and TO Si–O–Si surface phonons [17]. This is consistent with the excitation-energy independent PL lifetime of about 1 ns. These particular spectral features imply perfect monodispersity of the NH_2-SiNP sample. The NH_2-SiNPs were allowed to age for several weeks under ambient conditions. An amorphous SiO_x shell was formed on expense of the core [13], until the core size had reached a magic number of Si atoms [18]. The zero-phonon PL peak at 405 nm corresponds to a band gap of 3.06 eV and therewith to a nanoparticle size of 1 nm that matches the Si_{29} cluster [18]. The aminosilane ligands of the NH_2-SiNPs provide positive surface charges and high solubility in aqueous environment.

Fig. 2 depicts the TEM images of 3T3 cells and MCF-7 cells which were incubated with SiNPs or NH_2-SiNPs. Apparently, no TEM micrograph exhibits any evidence for an uptake mechanism such as endocytosis or pinocytosis. Because of their ultrasmall sizes the nanoparticles may cross the cell membrane either by diffusion or through carriers and transporters. The positively charged NH_2-SiNPs were embedded in the membranes of most cell structures such as the endoplasmatic reticulum, mitochondria or vesicles (Fig. 2A3 and B1). Inside the MCF-7 cells the NH_2-SiNPs accumulated also in the cytoplasm. On the other hand, SiNP agglomerates were visualized in the cytoplasm as well as in the membrane of cell organelles of both cell lines (Fig. 2A1). The SiNPs even reached the cell nucleus (Fig. 2A2).

The biocompatibility of the NH_2-SiNPs and SiNPs for the 3T3 (Fig. 3A) and MCF-7 cells (Fig. 3B) was assessed using the MTT assay. The relative cell viability (%) of the cells, incubated with either SiNPs or NH_2-SiNPs, was compared with medium containing APTES or TOAB. The surfactant APTES (92% for MCF-7 and 97% for 3T3) exerted no influence on the cell viability. In contrast, the detergent TOAB caused larger cellular damage (23% for MCF-7 and 38% for 3T3) as provoking cell-membrane permeability. The smallest values of cell viability were obtained for SiNP incubated 3T3 and

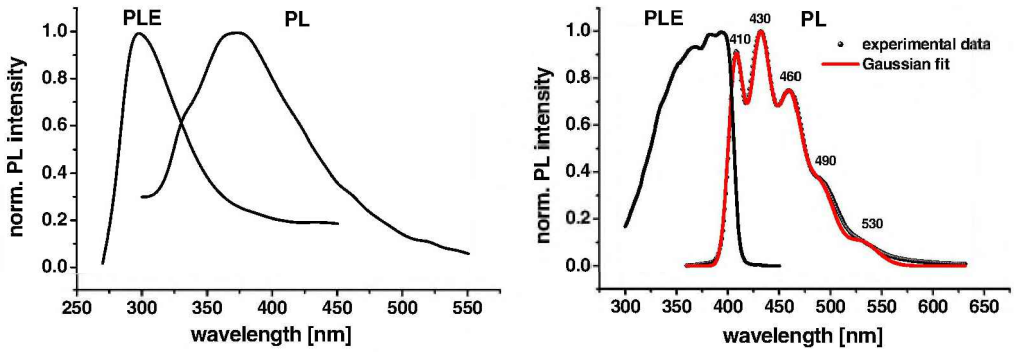

Fig. 1. Photoluminescence emission and excitation spectra of toluene colloids of SiNPs (left) and NH_2-SiNPs (right); the peak positions in the PL spectrum of the NH_2-SiNP colloid were obtained from a Gaussian fit of the experimental data (right panel, red line). (For interpretation of the references to color in this figure legend, the reader is referred to the web version of this article.)

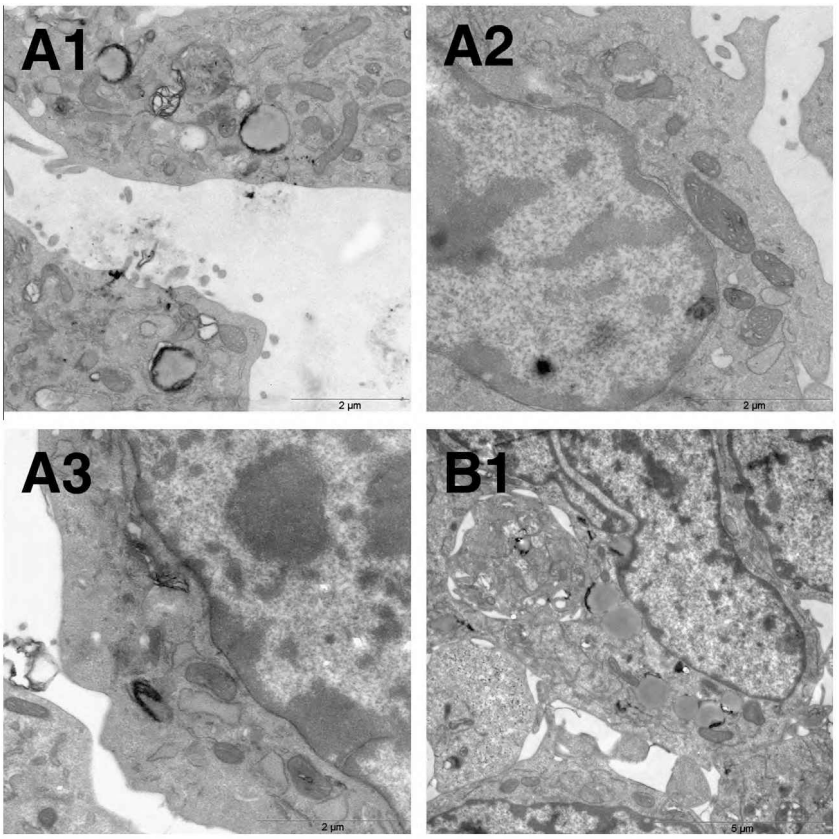

Fig. 2. TEM images of 3T3 (A) and MCF-7 (B) cells: SiNP agglomerates in the cytoplasm and cell organelle membranes (A1), the SiNPs reach the cell nucleolus (A2). NH_2-SiNPs in membranes of different cell structures (A3, B1), in the cytoplasm of MCF-7 cells (B1).

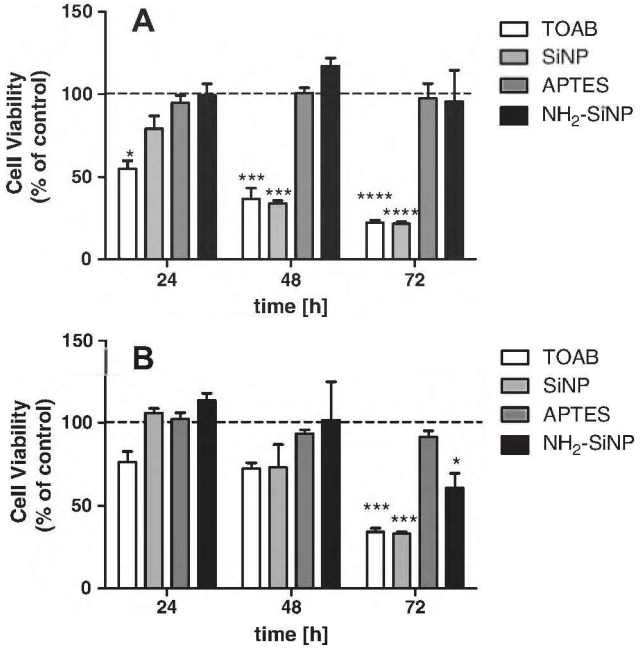

Fig. 3. Biocompatibility of the SiNPs was tested using the MTT Assay: the metabolic activity (%) of 3T3 (A) and MCF-7 (B) cells with TOAB, APTES, SiNPs or NH_2-SiNPs, $n = 6$, $^*p > 0.05$.

MCF-7 cells. This is explained with the penetration of the SiNPs into the cell nucleus, where they presumably damaged the DNA. The NH_2-SiNPs are insignificantly cytotoxic for 3T3 (Fig. 3A: 95% at 72 h) cells but less biocompatible for MCF-7 cells (Fig. 3B: 70% at 72 h).

To obtain complementary information of cytotoxicity for the silicon nanoparticles, the ROS and GSH concentration in MCF-7 and 3T3 cells were measured (Fig. 4A–C). The ROS may damage membranes through lipid peroxidation (LPO), in particular, when their formation takes place nearby membranes. Therefore the relative concentration of malondialdehyde (MDA), as being a LPO product, is determined for MCF-7 and 3T3 cells containing the silicon nanoparticles and for those without nanoparticles (Fig. 4D). The capability of the silicon nanoparticles to function as radiosensitizer was investigated by exposing SiNP and NH_2-SiNP incubated cells to X-radiation at a single dose of 3 Gy. The intracellular ROS concentration was subsequently measured using the DCF fluorescence dye assay (Fig. 4A and B). Even in non-irradiated cells the nanoparticles were observed to enhance the ROS formation: the SiNPs and NH_2-SiNPs raised the ROS concentration in 3T3 cells for 10% and in MCF-7 cells for 23% and 48%, respectively (Fig. 4A and B, blank columns). Obviously the increase of ROS formation is larger for the NH_2-SiNPs than for the SiNPs, and the NH_2-SiNP induced ROS formation is more efficient in tumor cells than in tissue cells. This is consistent with the results obtained from measuring the GSH concentration in MCF-7 and 3T3 cells (Fig. 4C). Compared to cells without nanoparticles (100%) the GSH level is drastically reduced for MCF-7 cells containing SiNPs (*ca.* 30%) or NH_2-SiNPs (*ca.* 30%) and significantly larger in 3T3 cells with SiNPs (55%) or NH_2-SiNPs (*ca.* 70%). Since a lowered GSH level is associated with an increased ROS concentration, these results clearly demonstrate that both, SiNPs and NH_2-SiNPs, enhanced the ROS production to a considerably larger extent in MCF-7 cells than in 3T3 cells. Under X-ray exposure the NH_2-

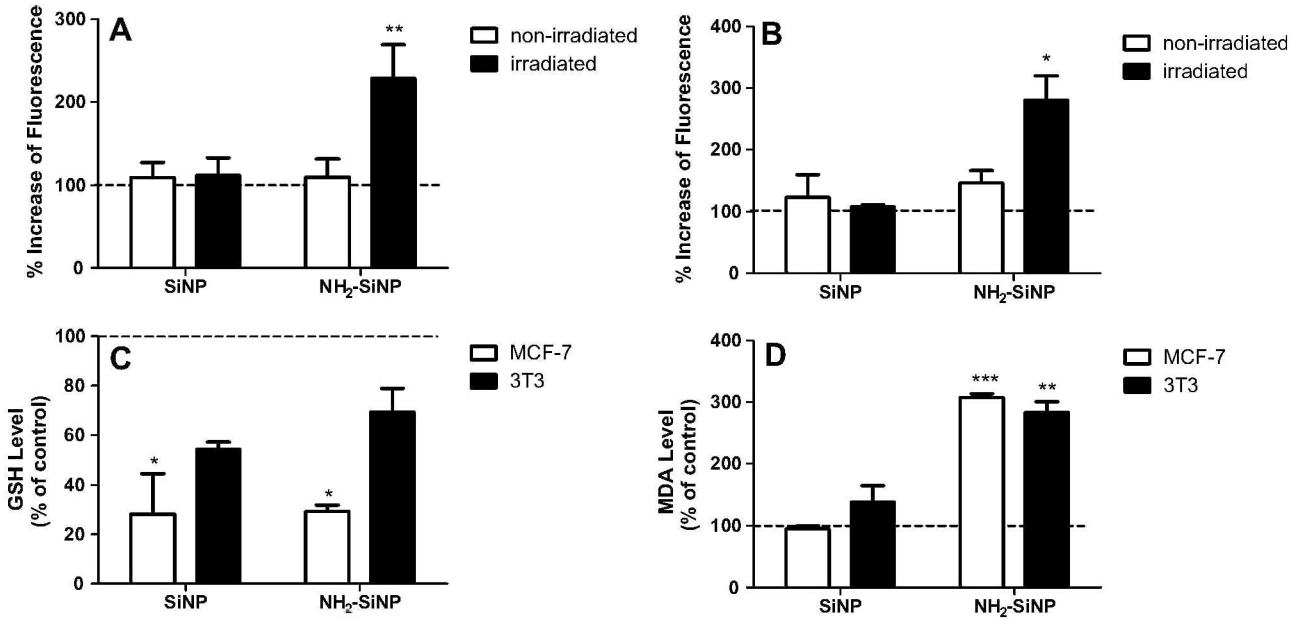

Fig. 4. Determination of the ROS concentration in 3T3 and MCF-7 cells containing SiNPs or NH_2-SiNPs before and after X-ray treatment: the relative ROS concentration in 3T3 (A) and MCF-7 (B) cells scales with the relative DCF fluorescence intensity (%), $n = 6$, $^*p > 0.05$; GSH Level (C) in non-irradiated cells, $n = 2$, $^*p > 0.05$; MDA level (D) in SiNP or NH_2-SiNP loaded cells after X-ray treatment, $n = 2$, $^*p > 0.05$.

SiNP incubated 3T3 and MCF-7 cells exhibited a rise of ROS concentration to 120% and 180%, respectively, whereas the impact of X-radiation on the ROS formation was negligibly small for these cells with internalized SiNPs (Fig. 4A and B, black columns). This may arose from differences in the surface architectures and charges of the SiNPs and NH_2-SiNPs. The SiNPs agglomerated in the cytoplasm and various cell organelle membranes. In contrast, the NH_2-SiNPs were predominantly incorporated in the mitochondrial membrane, where they may induce oxidative stress and thereupon, provide the ROS formation when interacting with X-rays. In order to examine the effect of the silicon nanoparticle-induced ROS production on the membranes in X-ray treated cells, the relative MDA concentration, as scaling the LPO, was measured (Fig. 4D). For both, the MCF-7 and 3T3 cells, when containing NH_2-SiNPs, the MDA level rose to 200%. This significant increase most likely resulted from efficient membrane LPO due to mitochondrial ROS formation. By comparison, the SiNPs raised the MDA level for 50% in 3T3 cells, and did not affect the membranes in MCF-7 cells.

4. Discussion

The applicability of SiNPs and NH_2-SiNPs as radiosensitizer in tumor cells was assessed by examining the impact of X-rays on the ROS formation in MCF-7 and 3T3 cells. Information of the nanoparticle sizes were obtained from PL spectroscopy data. The NH_2-SiNP sample is monodisperse. The Si core size is about 1 nm and is therewith assigned to the Si_{29} cluster. The amino groups of the NH_2-SiNPs provide positive surface charges in the cytosol, which facilitate their accumulation in membranes of the endoplasmatic reticulum, mitochondria and vesicles. On the other hand, the freshly synthesized SiNPs exhibited a broad size distribution around 1 nm. The SiNPs formed agglomerates in the cytosol and membranes as well as were visualized to reach the cell nucleus, where they caused DNA-damage induced apoptosis. The latter is evident from cell viability measurements: the 72 h value of the relative cell viability is decreased to 23% and 30% for 3T3 and MCF-7 cells, respectively. By comparison, the NH_2-SiNPs, as being observed to accumulate in mitochondrial membranes, are expected to provide an increased mitochondrial metabolism that should provoke oxidative stress and thus the generation of ROS. Cancer cells like MCF-7 cells have in general a higher metabolic activity than normal cells like 3T3. This explains the observed higher ROS concentration for NH_2-SiNPs loaded MCF-7 cells in comparison with 3T3 cells that contained these nanoparticles. This result was confirmed by the measurement of the intracellular concentration of GSH which is considerably smaller for the MCF-7 cells than for the 3T3 cells. Additional validation was obtained from cell viability measurements using the MTT assay as assessing the mitochondrial function via the mitochondrial dehydrogenase. Under X-ray exposure the NH_2-SiNPs increased the ROS concentration in 3T3 cells for 120% and in MCF-7 cells for 180%. The impact of X-rays onto the mitochondrial membrane is the depolarization of the latter. Membrane depolarization may open the permeability transition pores and thereupon, enables the cytochrome-c release into the cytoplasm. The release of cytochrome-c triggers the accumulation of ROS, which increases the oxidation state of the cell. Additionally inhibition of the respiratory chain raises the ubisemiquinone free radical level in the catalytic mechanism of complex III (ubiquinol/cytochrome-c oxido-reductase). The ubiquinone site in complex III catalyzes the conversion of molecular oxygen to the superoxide anion radical [19]. The NH_2-SiNPs, as being embedded in the outer mitochondrial membrane and definitely increasing the ROS formation, evidently enhance the depolarizing effect of the X-radiation on the mitochondria. This implies that the radiosensitizing effect of the NH_2-SiNPs principally arises from their active involvement in the mitochondrial metabolism. We may conclude that ultrasmall NH_2-SiNPs negligibly affect the cell viability and are thus suited as radiosensitizer for X-radiation in tumor cells, even though the enhancing effect is limited to the mitochondrial ROS production.

Acknowledgments

Support of the Deutsche Forschungsgemeinschaft (graduate school 1161/2) is gratefully acknowledged. We thank Andrea

Hilpert for TEM imaging studies (Institute of Anatomy I, Friedrich-Alexander University of Erlangen-Nuremberg). Sincere thanks are given to PD Dr. Oliver Zolk (Institute of Clinical Pharmacology and Toxicology, Friedrich-Alexander University of Erlangen-Nuremberg) for generously supporting our cell viability assay experiments. Furthermore, we are grateful to Andreas Postatny for conducting so diligently the ICP-AES experiments on our samples. (Prof. Dr. Peter Wasserscheid, CRT, Friedrich-Alexander University of Erlangen-Nuremberg). M.L.D and M.C.G. are research members of CONICET, Argentina. The authors thank DAAD (PROALAR 54365954, Germany) and MINCYT (Argentina) for a collaborative project.

References

[1] D. Kovalev, M. Fujii, Silicon nanocrystals: photosensitizers for oxygen molecules, Adv. Mater. 17 (2005) 2531–2544.
[2] L.A. Osminkina, K.P. Tamarov, A.P. Sviridov, R.A. Galkin, M.B. Gongalsky, V.V. Solovyev, A.A. Kudryavtsev, V.Y. Timoshenko, Photoluminescent biocompatible silicon nanoparticles for cancer theranostic applications, J. Biophotonics 5 (2012) 529–535.
[3] P. Juzenas, W. Chen, Y.P. Sun, M.A.N. Coelho, R. Generalov, N. Generalova, I.L. Christensen, Quantum dots and nanoparticles for photodynamic and radiation therapies of cancer, Adv. Drug Deliv. Rev. 60 (2008) 1600–1614.
[4] P.M. David Gara, N.I. Garabano, M.J. Llansola Portolés, M.S. Moreno, D. Dodat, O.R. Casas, M.C. Gonzalez, M.L. Kotler, ROS enhancement by silicon nanoparticles in X-ray irradiated aqueous suspensions and in glioma C6 cells, J. Nanopart. Res. 14 (2012) 741-1–741-13.
[5] J. Ahmad, M. Ahamed, M.J. Akhtar, S.A. Alokayan, M.A. Siddiqui, J. Musarrat, A.A. Al-Khedhairy, Apoptosis induction by silica nanoparticles mediated through reactive oxygen species in human liver cell line HepG2, Toxicol. Appl. Pharmacol. 259 (2012) 160–168.
[6] T. Morishige, Y. Yoshioka, H. Inakura, A. Tanabe, X. Yao, S. Narimatsu, Y. Monobe, T. Imazawa, S. Tsunoda, Y. Tsutsumi, Y. Mukai, N. Okada, S. Nakagawa, The effect of surface modification of amorphous silica particles on NLRP3 inflammasome mediated IL-1β production, ROS production and endosomal rupture, Biomaterials 31 (2010) 6833–6842.
[7] B. Fubini, A. Hubbard, Reactive oxygen species (ROS) and reactive nitrogen species (RNS) generation by silica in inflammation and fibrosis, Free Radical Biol. Med. 34 (2003) 1507–1516.
[8] K.-A. Kim, Y.-H. Kim, M.S. Seo, W.K. Lee, S.W. Kim, H. Kim, K.-H. Lee, I.-C. Shin, J.-S. Han, H.J. Kim, Y. Lim, Mechanism of silica-induced ROS generation in Rat2 fibroblast cells, Toxicol. Lett. 135 (2002) 185–191.
[9] E.Yu. Bryleva, N.A. Vodolazkaya, N.O. Mchedlov-Petrossyan, L.V. Samokhina, N.A. Matveevskaya, A.V. Tolmachev, Interfacial properties of cetyltrimethylammonium-coated SiO2 nanoparticles in aqueous media as studied by using different indicator dyes, J. Colloid Interface Sci. 316 (2007) 712–722.
[10] F. Erogbogbo, K.T. Yong, I. Roy, G.-X. Xu, P.N. Prasad, M.T. Swihart, Biocompatible luminescent silicon quantum dots for imaging of cancer cells, ACS Nano 2 (2008) 873–878.
[11] L. Ruizendaal, S. Bhattacharjee, K. Pournazari, M. Rosso-Vasic, L.H.J. de Haan, G.M. Alink, A.T.M. Marcelis, H. Zuilhof, Synthesis and cytotoxicity of silicon nanoparticles with covalently attached organic monolayers, Nanotoxicology 3 (2009) 339–347.
[12] S. Bhattacharjee, L.H.J. de Haan, N.M. Evers, X. Jiang, A.T.M. Marcelis, H. Zuilhof, I.M.C.M. Rietjens, G.M. Alink, Role of surface charge and oxidative stress in cytotoxicity of organic monolayer-coated silicon nanoparticles towards macrophage NR8383 cells, Part. Fibre Toxicol. 7 (2010) 25-1–25-12.
[13] M.J. Llansola Portolés, R. Pis Diez, M.L. Dell'Arciprete, P. Caregnato, J.J. Romero, D.O. Martire, O. Azzaroni, M. Ceolín, M.C. Gonzalez, Understanding the parameters affecting the photoluminescence of silicon nanoparticles, J. Phys. Chem. C 116 (2012) 11315–11325.
[14] H. Ohkawa, N. Ohishi, K. Yagi, Assay for lipid peroxides in animal tissues by thiobarbituric acid reaction, Anal. Biochem. 95 (1979) 351–358.
[15] G.I. Ellman, Tissue sulfhydryl groups, Arch. Biochem. Biophys. 82 (1959) 70–77.
[16] M.V. Wolkin, J. Jorne, P.M. Fauchet, G. Allan, C. Delerue, Electronic states and luminescence in porous silicon quantum dots: the role of oxygen, Phys. Rev. Lett. 82 (1999) 197–200.
[17] J. Martin, F. Cichos, F. Huisken, C. von Borczyskowski, Electron-phonon coupling and localization of excitons in single silicon nanocrystals, Nano Lett. 8 (2008) 656–660.
[18] G. Belomoin, J. Therrien, A.D. Smith, S. Rao, R.D. Twesten, S. Chaieb, M. Nayfeh, L. Wagner, L. Mitas, Observation of a magic discrete family of ultrabright Si nanoparticles, Appl. Phys. Lett. 80 (2002) 841–843.
[19] C. Fleury, B. Mignotte, J.L. Vayssière, Mitochondrial reactive oxygen species in cell death signaling, Biochimie 84 (2002) 131–141.